JOURNAL OF SOLID STATE CHEMISTRY 81, 83–95 (1989)

A Study of the Oxygen-Deficient Perovskite $Ba_{1-x}La_xFeO_{3-y}$ by Mössbauer Spectroscopy

T. C. GIBB* AND M. MATSUO

Department of Inorganic and Structural Chemistry, The University, Leeds LS2 9JT, England

Received September 26, 1988; in revised form February 28, 1989

The oxygen-deficient perovskite system $Ba_{1-x}La_xFeO_{3-y}$ ($0 \leq y \leq 0.5$) has been studied by Mössbauer spectroscopy and X-ray powder diffraction techniques. The value of y depends strongly on the conditions of preparation, but the materials remain a cubic peroskite for $0.1 \leq x < 0.8$. For small y there is a nominal charge disproportionation $2Fe^{4+} \rightleftharpoons Fe^{3+} + Fe^{5+}$ with decreasing temperature which is related to the onset of magnetic ordering. For large y (~0.5) there is no evidence for the existence of the ordered-vacancy structures which are known to exist for the Ca/La and Sr/La systems. By analogy with similar Sr/rare-earth systems it is proposed that the cubic phase has a macroscopic perovskite structure with magnetic coherence throughout the lattice. The oxygen vacancies can partially order into alternate FeO_2 layers to form a coherent intergrowth of microdomains. © 1989 Academic Press, Inc.

Introduction

There have been many studies of the magnetic and electronic properties of those mixed-metal oxides which are structurally related to the mineral perovskite, $CaTiO_3$. This structure has the ability to stabilize cations in unusually high oxidation states, and the anion sublattice can accommodate a high concentration of vacant sites. The recent discovery (*1*) of superconductivity in the so-called 1:2:3 compound $YBa_2Cu_3O_{7-y}$, which is an oxygen-deficient perovskite, has magnified the interest in these materials.

The related 1:2:3 iron compounds, more usually written as $A_2BFe_3O_{8+y}$, have also excited considerable interest, although for different reasons. Stoichiometric $Ca_2LaFe_3O_8$ can be prepared (*2–4*) by standard ceramic techniques under flowing argon at 1100°C. The structure is almost certainly derived from the cubic perovskite by an ordered arrangement of oxygen vacancies along [101] axes to give an orthorhombic unit cell with layers of iron cations in tetrahedral coordination, each separated by two layers of iron in octahedral coordination to oxygen. It has also been described as the $n = 3$ term in a general series $A_nB_nO_{3n-1}$ intermediate between ABO_3 ($n = \infty$, perovskite) and $A_2B_2O_5$ ($n = 2$, brownmillerite) in which different structural motifs in various proportions intergrow coherently along one direction. High-resolution electron micrographs (*5–7*) have shown the possibility for coherent intergrowth of the $Ca_2Fe_2O_5$ and $Ca_2LaFe_3O_8$ lattices, and it is clear that $Ca_2LaFe_3O_8$ is one ideal composition in a solid solution in which the composition is

* To whom correspondence should be addressed.

0022-4596/89 $3.00

Copyright © 1989 by Academic Press, Inc.
All rights of reproduction in any form reserved.

changed by altering the relative numbers of octahedral and tetrahedral layers. Quenching $Ca_2LaFe_3O_8$ from 1400°C in air produces a "cubic" perovskite phase (*3*) which contains a microdomain texture with an intergrowth of small domains of the order of ~60–100 Å across in size, related to the orthorhombic $Ca_2LaFe_3O_8$ structure, but randomly oriented along each of the three cubic directions.

Work on the brownmillerite Sr_2CoFeO_5 in our laboratory (*8*) using Mössbauer spectroscopy as the main technique has shown that microdomains can also be produced in this compound by quenching in air from 1400°C, while they are absent if the compound is quenched into liquid nitrogen. Rapid oxidation takes place to produce small nonequilibrium microdomains with excess oxygen incorporated in the domain walls. A parallel investigation (*9*) of $Ca_2LaFe_3O_8$ confirmed that the oxidation is largely a product of the quench itself. It has been proposed that the high-temperature cubic phase of $Sr_2Fe_2O_5$ also contains microdomains of the low-temperature brownmillerite phase (*10*).

A major study of the $Sr_2LaFe_3O_{8+y}$ system has also proved fruitful (*11–13*). A cubic phase with $0.6 < y < 1$ shows (*11*) a first-order transition from a high-temperature paramagnetic averaged-valence state in which all Fe cations are electronically equivalent to a low-temperature antiferromagnetic mixed-valence state by the nominal charge disproportionation $2Fe^{4+} \rightleftharpoons Fe^{3+} + Fe^{5+}$. In the range $(0 < y < 0.6)$ three new ordered vacancy phases were found (*12, 13*). Orthorhombic $Sr_2LaFe_3O_8$ is an antiferromagnet (T_N = 715 K) and is analogous to $Ca_2LaFe_3O_8$. A second high-temperature form of $Sr_2LaFe_3O_8$ has a doubled cubic perovskite cell which is thought to derive from a partial ordering of oxygen vacancies into alternate FeO_2 layers perpendicular to $[100]_c$. The third phase appears to have a range of stoichiometry below the ideal composition $Sr_2LaFe_3O_{8.5}$, orders antiferromagnetically at 500 K, and is believed to be related to the mixed-valence phase $SrFeO_{2.75}$.

An extension of the work (*13*) to include the other rare earths ($Sr_2MFe_3O_{8+y}$, M = La, Ce, Pr, Nd, Sm, Eu, Gd, Dy, Er, Yb, and Y) revealed that the tendency to oxidation decreases rapidly across the series. An additional cubic phase was isolated for elements in the middle of the series. It was concluded that this cubic phase has a macroscopic perovskite structure in which oxygen vacancies are partially ordered into alternate FeO_2 layers to form a coherent intergrowth of microdomains, but with magnetic coherence throughout the lattice. The phase is thermodynamically unstable at low temperatures with respect to the orthorhombic phase with ordered vacancies, but for kinetic reasons the latter is not always achieved. Rapid oxidation during cooling takes place initially along microdomain boundaries and thereby destroys the long-range spin coherence.

A logical extension of this work was to investigate the corresponding $Ba_2LaFe_3O_{8+y}$ system which had not been examined hithertoo. In the event, we were unable to produce the ordered defect phases found for Ca and Sr, and accordingly expanded the study to encompass the whole $Ba_{1-x}La_xFeO_{3-y}$ solid solution. A paper published (*14*) after the work had been completed which complimented our results describes electron microscopy results on the same system, and has proved useful in the discussion.

Experimental

Accurately weighed amounts of spectroscopic grade Fe_2O_3, $BaCO_3$, and La_2O_3, with stoichiometric ratios appropriate for $Ba_{1-x}La_xFeO_{3-y}$ were ground together in a ball mill, pressed into a pellet, and initially fired in a platinum crucible at 1300°C for 4–

7 days with two intermediate grindings before quenching onto a metal plate in air. Aliquots of this material were then treated in several different ways: annealing in air at 1300°C for about 3 days before quenching in air or into liquid nitrogen, or slow cooling in air to room temperature; annealing in argon for 4–5 days at 1200°C before slowly cooling at 50° per hour to room temperature; annealing *in vacuo* (10^{-4} Torr) at 1000°C. Initial characterization in each case was by X-ray powder diffraction recorded with a Philips diffractometer using nickel-filtered Cu$K\alpha$ radiation. All the cubic components reported here gave sharp X-ray patterns with no impurity lines (there was no evidence of any reaction with the Pt crucibles). Chemical analyses for nominal Fe^{4+} content were carried out by digestion in a standardized solution of ammonium iron (II) sulfate in the presence of HCl and titration with cerium(IV) sulfate using ferroin as indicator.

Mössbauer data were collected in the temperature range $4.2 < T < 723$ K using a ^{57}Co/Rh source matrix held at room temperature; isomer shifts were determined relative to the spectrum of metallic iron.

Results

Samples of $Ba_{1-x}La_xFeO_{3-y}$ were prepared for $x = 0, 0.10, 0.20, 0.33, 0.50, 0.67, 0.80$, and 0.90 under carefully controlled conditions as described above. A fast quench into liquid nitrogen from 1300°C was employed to prevent rapid oxidation during cooling, a problem which is common to several related systems (*8, 9, 11–13*). Alternatively, the sample was slowly cooled in air from 1300°C at 25° per hour to maximize the oxygen uptake. The values for y are given in Table I and are also plotted in Fig. 1, together with the data of Parras *et al.* (*14*) which refer to samples quenched in air in an alumina crucible. It is clear that quenching in air is accompanied by rapid oxygen uptake, the final value of y depending on many factors such as sample size. Indeed where we have carried out a corresponding quench in a platinum crucible onto a large metal plate, the oxidation achieved was generally much less, e.g., for $x = 0.33$, $y = 0.272$. The X-ray powder pattern suggested that the sample was very inhomogeneous, and this was consistent with the Mössbauer spectra. The oxygen deficit is very small for $x > 0.6$ in the slowly cooled samples.

TABLE I

THE OXYGEN PARAMETER y AND X-RAY LATTICE PARAMETER a FOR THE SOLID SOLUTIONS $Ba_{1-x}La_xFeO_{3-y}$ PREPARED AT 1300°C IN AIR AND EITHER SLOW-COOLED OR QUENCHED INTO LIQUID NITROGEN

	Slow-cooled		Quenched	
x	y	a (Å)	y	a (Å)
0	0.213	6H-hexagonal	0.487	Monoclinic
0.10	0.329	3.997	0.438	4.038
0.20	0.213	3.966	0.386	4.011
0.33	0.113	3.939	0.290	3.979
0.50	0.030	3.929	0.216	3.951
0.67	0.026	3.922	0.106	3.930
0.80	0.00	(3.92)	0.045	(3.92)
0.90	—	Orthorhombic	0.00	Orthorhombic

Although it was not the intention to study the $BaFeO_{3-y}$ system ($x = 0$) in detail, samples of this material were prepared under the same conditions as the solid solutions for comparison purposes. The structural chemistry of $BaFeO_{3-y}$ is unusually complex with at least eight different forms being identified in early work (*15–20*). Several of these forms may not be thermodynamically stable, and the overall phase diagram remains obscure. The principal phase is a 6H-hexagonal phase which appears to exist for $0.05 < y < 0.37$ (*18, 21*), a very wide composition range. This is in contrast to the $SrFeO_{3-y}$ system which has four phases over the same composition range, all derived from cubic close-packing (*22*). A neutron diffraction study (*23*) of 6H-$BaFeO_{2.79}$

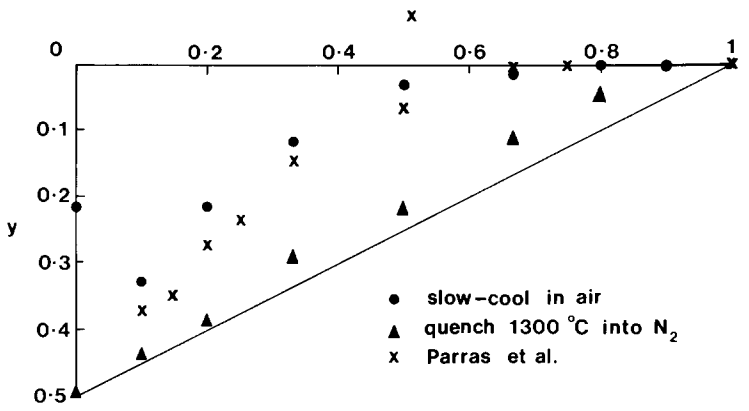

FIG. 1. The compositional region for $Ba_{1-x}La_xFeO_{3-y}$ showing the samples described in this work and by Parras *et al.* (*14*).

shows it to have the barium titanate structure: pairs of octahedral Fe sites share faces and are linked by octahedral Fe sites with only corner sharing. The oxygen vacancies are mainly in the shared faces. Electron diffraction lattice images (*24*) have shown that stacking faults can occur, but are not thought to have a significant bearing on the vacancy concentration. At 1000°C in nitrogen the compound with $y = 0.50$, i.e., $Ba_2Fe_2O_5$, is cubic (*18*), but this transforms on cooling in the absence of oxygen to a phase which was initially mistaken for a brownmillerite (*16, 17*), and has since been variously described as triclinic (*18–20*), orthorhombic (*25*), and more recently monoclinic (*26*). The Mössbauer spectra (*16, 20*) are compatible with a structure perhaps related to the simpler brownmillerite type of lattice, which has equal numbers of Fe^{3+} cations in octahedral and tetrahedral coordination to oxygen as in $Ca_2Fe_2O_5$ and $Sr_2Fe_2O_5$, but distorted so as to generate at least four distinct sites in a much enlarged unit cell.

In the present work the sample prepared by slow-cooling in air from 1300°C gave an X-ray pattern which could be indexed as the 6H-hexagonal phase. That quenched from 1300°C into liquid nitrogen was indexed as the monoclinic phase (*26*). In the event, substitution of only 10% lanthanum produced a new cubic phase, and the two-phase mixtures of cubic perovskite and monoclinic $Ba_2Fe_2O_5$ (reported recently (*14*) for $x = 0.10$, 0.15, 0.20, and 0.25 quenched in air) were not found. For $0.1 \leq x \leq 0.67$ both the quenched and slow-cooled sample were a cubic perovskite with sharp X-ray lines. There was also a very diffuse reflection at a d-spacing of ~5.5 Å ($\sqrt{2}a$) which is attributed to short-range ordering (see below). The lattice parameter (Table I) decreases uniformly with increasing La content and with decreasing oxygen vacancy concentration. For $x = 0.8$ the pattern was still essentially cubic but the high-angle lines were broader with some degree of splitting which was more pronounced in the oxidized sample. For $x = 0.9$, the pattern showed additional lines and could be indexed as an orthorhombic lattice of the $LaFeO_3$ type (*27*). It is noteworthy that the cubic system was found over a wider composition range than by Parras *et al.* (*14*). They appear to have fired their materials only once, and it is possible that the repeated firings used here give a more homo-

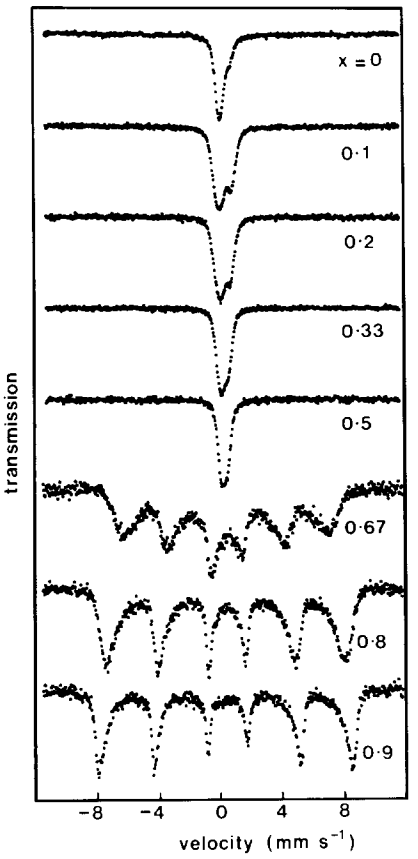

FIG. 2. The Mössbauer spectra at 290 K for samples of $Ba_{1-x}La_xFeO_{3-y}$ slow-cooled in air from 1300°C.

geneous material. The large size difference between Ba^{2+} and La^{3+} may result in long times for diffusion and equilibration of these cations in ceramic preparations.

Considerable effort was expended in an attempt to produce materials at $x = 0.33$ with ordered oxygen vacancies in a perovskite supercell. Despite the use of various heat treatments including annealing under argon at 1200°C and then at successively lower temperatures, no trace was found of an orthorhombic $Ba_2LaFe_3O_8$ phase, and thus the Ba/La system differs markedly from the Ca/La and Sr/La systems where ordered defect phases occur readily.

Mössbauer Spectra of Samples Slow-Cooled in Air

The Mössbauer spectra at 290 K for the samples slowly cooled in air are shown in Fig. 2. The cubic solid-solution remains paramagnetic at this temperature until $x > 0.5$, and the 6H-phase ($x = 0$) is also paramagnetic. The asymmetry in the spectra is indicative of mixed valence states. For $x \geq 0.67$ the system is magnetically ordered, the sharpening of the lines and the greater overall span as x increases being consistent with a rising critical temperature.

The temperature dependence of the spectrum of $BaFeO_{2.787}$ is shown in Fig. 3. The critical temperature for magnetic order is very indistinct, but appears to be at least 140 K. The spectrum is very broad at 78 K, but at 4.2 K shows a comparatively sharp magnetic hyperfine pattern. This can be represented by two hyperfine fields with flux densities of 49.0 and 24.8 T, respectively, without any quadrupole perturbation but with broadened lines (see Table II). The isomer shift, δ, and flux density, B, of the first component are consistent with the Fe^{3+} valence state. The other component is consistent with the Fe^{5+} valence state. The observed area ratios compare favorably with the nominal distribution of oxidation states calculated on this basis from the oxygen analysis, but disagree with the alternative of Fe^{3+}/Fe^{4+}.

TABLE II

MÖSSBAUER PARAMETERS FOR SLOW-COOLED SAMPLES OF $Ba_{1-x}La_xFeO_{3-y}$ AT 4.2 AND 290 K

							Nominal values	
x	y	T (K)	B (T)	δ (mm sec^{-1})	Δ (mm sec^{-1})	%	%Fe^{4+}	%Fe^{5+}
0	0.213	4.2	49.0	0.46	—	73		
			24.8	−0.13	—	27	58	29
		290	—	0.44	0.43	37		
			—	−0.05	0.17	63	58	29
0.5	0.030	4.2	51.0	0.43	—	78		
			27.1	0.01	—	22	44	22
		290	—	0.28	0.39	62		
			—	0.10	0.35	38	44	22

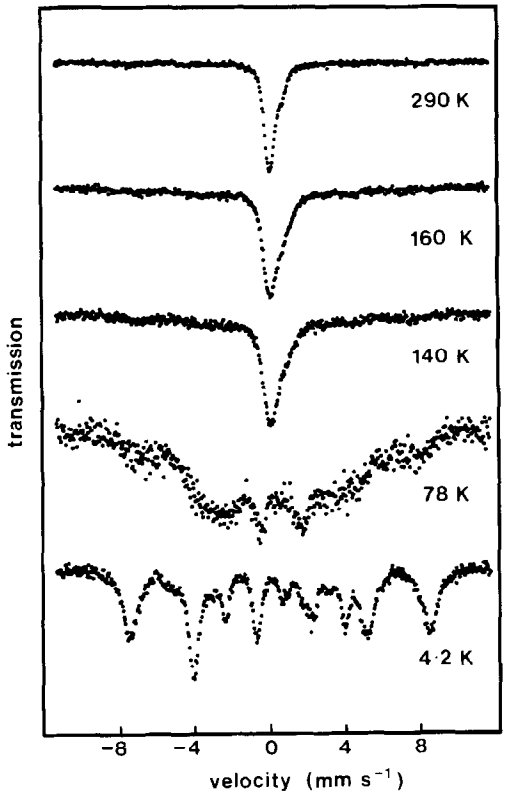

FIG. 3. The Mössbauer spectrum of 6H-$BaFeO_{2.787}$ as a function of temperature.

TABLE III

THE MAGNETIC FLUX DENSITIES, B, IN TESLA AT 4.2 K FOR COMPOUNDS SHOWING CHARGE DISPROPORTIONATION

Compound	B (Fe^{3+})	B (Fe^{5+})	B (average)	Ref.
$CaFeO_3$	41.6	27.9	34.8	(*28*)
$SrFeO_3$	—	—	33.1	(*31*)
$Ca_{0.5}La_{0.5}FeO_{2.93}$	51.7	26.6	39.1	(*29*)
$Sr_2LaFe_3O_{8.94}$ (78 K)	45.1	25.9	35.5	(*11*)
$Sr_{0.7}La_{0.3}FeO_3$	46.0	26.9	36.5	(*30*)
6H-$BaFeO_{3-y}$	48.2	24.0	36.1	(*20*)
6H-$BaFeO_{2.787}$	49.0	24.8	36.9	This work
$Ba_{0.5}La_{0.5}FeO_{2.970}$	51.0	27.1	39.1	This work

The disproportionation of Fe^{4+} into nominally Fe^{3+} and Fe^{5+} was first discovered in $CaFeO_3$ (*28*) following which it was also suggested that the existing data for $BaFeO_{3-y}$ by Gallagher *et al.* (*16*) and Ichida (*20*) might be interpreted in the same way. The values for the flux density, with the averaged values for $CaFeO_3$ and other similar systems involving Ca/La (*29*) and Sr/La (*11, 30*) are shown in Table III. They are all distinctly different from $SrFeO_3$ which shows only a single hyperfine field from Fe^{4+} of 33.1 T (*31*). Although the values for the isomer shifts and flux densities of the two fields vary, the average values are comparatively close to each other. This is probably a reflection of the degree of charge separation which takes place; the final result is not necessarily integral charge states, a fact which has been clearly established in the Sr/La and Sr/Ca solid solutions (*30*). In conclusion, the charge disproportionation in $BaFeO_{2.787}$ is clearly established. The coexistence of disproportionation and high oxygen deficiency is

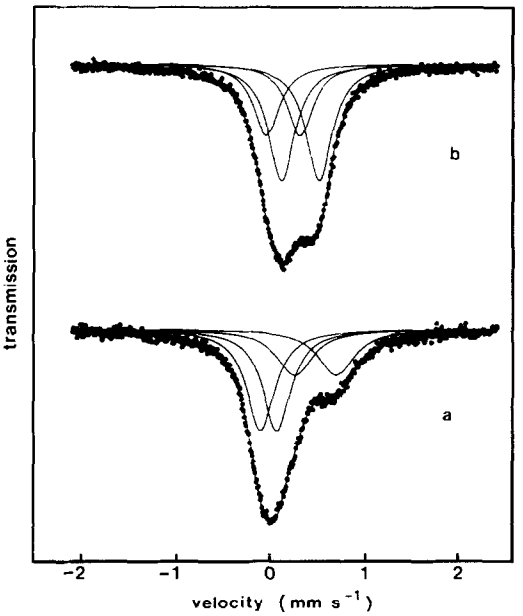

FIG. 4. The Mössbauer spectrum at 290 K of (a) 6H-$BaFeO_{2.787}$ and (b) $Ba_{0.5}La_{0.5}FeO_{2.970}$ showing the computed analysis in terms of two quadrupole doublets.

interesting, and we are in the process of obtaining neutron diffraction data at low temperatures to study this feature more closely.

The paramagnetic spectra for $x = 0$ and 0.50 taken over a reduced velocity range are shown in Fig. 4. All the paramagnetic spectra can be fitted quite well using a simple model with two overlapping symmetrical quadrupole doublets, but for reasons explained below the results must be treated with circumspection. We shall initially consider the case of $x = 0$. The isomer shift at 290 K given in Table II for the component at lower velocity is clearly anomalous with regard to the expected negative second-order Doppler shift with rise in temperature, and shows that a fast electron transfer has caused an effective change in the valence state. A similar behavior is well established in the Sr/La system (*11, 30*), where we have shown that the Mössbauer spectra of $Sr_2LaFe_3O_{8.94}$ show complete averaging of the Fe oxidation state. However, evidence was found for a degree of electron trapping as the oxygen vacancy concentration increased. $BaFeO_{2.787}$ contains nominally 58% Fe^{4+}, and this corresponds very well with the computed area of the component at more negative velocity. It thus seems reasonable to suggest that $BaFeO_{2.787}$ behaves as a mixed-valence Fe^{3+}/Fe^{5+} material at 4.2 K and as a mixed-valence Fe^{3+}/Fe^{4+} material at 290 K. However, the possibility remains that the electrons are not completely localized at 290 K, and, together with the added complication of the existence of two distinct sites in the 6H-structure, leads us to recommend caution in taking the results from the computer fit too literally. However, the asymmetry of the spectrum effectively constrains the proportions of the two valence states. It is not easy to define the temperature at which the change in valence states takes place, although the grossly broadened magnetic spectra above 78 K may reflect an increasing mobility of the electrons. It is worth noting that in $BaFeO_{2.95}$ there is a large anomaly in the magnetization immediately below the ordering temperature (*16, 19*), and we suggest that the change in valence states is closely associated with the onset of magnetic ordering as it is in $Sr_2LaFe_3O_{8.94}$ (*11*). The structural implications of this charge disproportionation in 6H-$BaFeO_{3-y}$ are currently under further investigation.

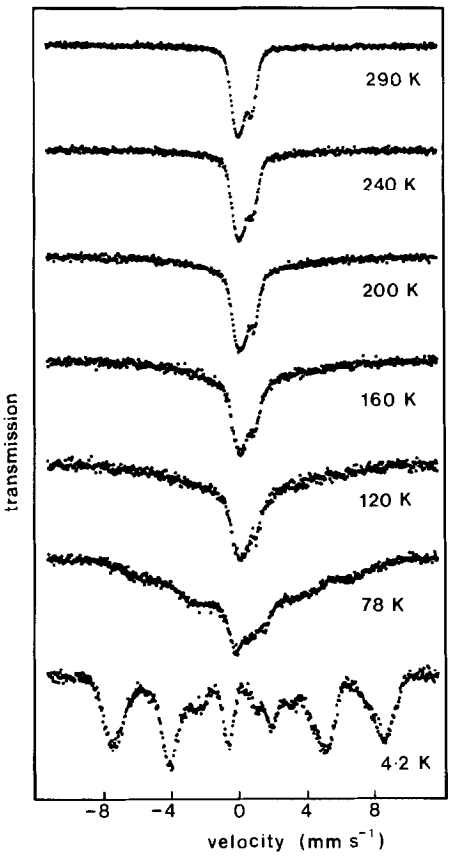

FIG. 5. The Mössbauer spectrum of $Ba_{0.9}La_{0.1}FeO_{2.671}$ as a function of temperature.

The Mössbauer spectrum as a function of temperature for the slow-cooled cubic samples with $x = 0.10$, 0.20, 0.33, and 0.50 are shown in Figs. 5–8, respectively. At 4.2 K the spectrum for $x = 0.50$ is comparatively sharp and similar to that for $BaFeO_{2.787}$. It

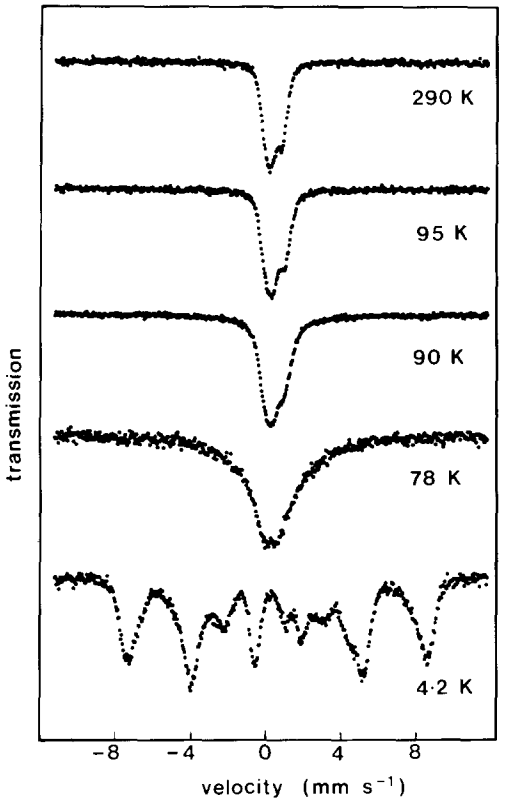

FIG. 6. The Mössbauer spectrum of $Ba_{0.8}La_{0.2}FeO_{2.787}$ as a function of temperature.

can be analyzed as two hyperfine fields with flux densities of 51.0 and 27.1 T (see Table II), but without any quadrupole perturbation. It is evident that there is a charge disproportionation into Fe^{3+} and Fe^{5+} in the cubic phase. The low vacancy concentration in this sample results in a nominal Fe^{5+} content of 22%, which agrees well with the computed area ratio. The spectrum at 290 K (Fig. 4b) can be analyzed as two quadrupole doublets, the area ratios now being appropriate to a description in terms of Fe^{3+}/Fe^{4+}, although once again the simplistic model may not be entirely appropriate. Regardless of the model, the isomer shift of any low oxidation state must be anomalous with respect to the value at 4.2 K, indicative of an effective change in oxidation state. From Fig. 8 it can be seen that magnetic hyperfine splitting commences at circa 250 K, but that there is still some degree of relaxational collapse at 150 K.

The spectra at 4.2 K for $x = 0.10$, 0.20, and 0.33 (Figs. 5–7) are clearly similar to that for $x = 0.50$, signifying that charge disproportionation is occurring, but the lines are broader. Computer fits to the data on the basis of two hyperfine fields overestimate the fraction of Fe^{5+}, but this is probably because the model does not correctly represent the line shapes. There may also be some degree of inward collapse in the spectra which weights the apparent contribution from the inner component. There is

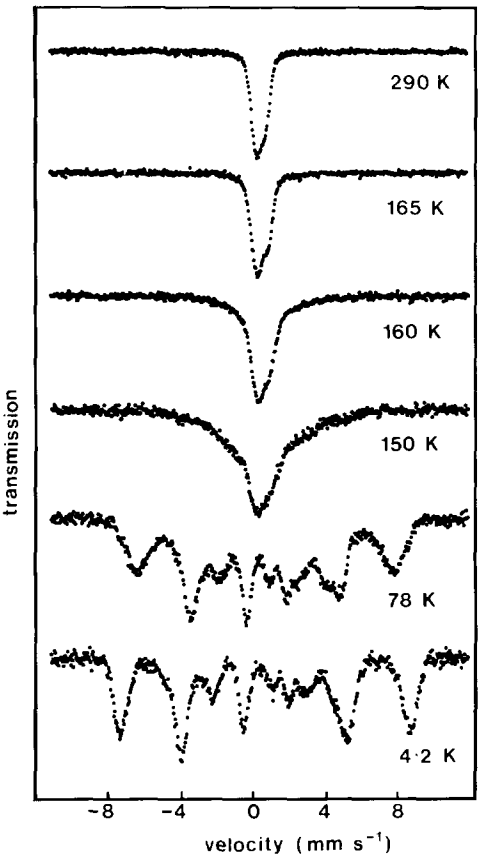

FIG. 7. The Mössbauer spectrum of $Ba_{0.67}La_{0.33}FeO_{2.887}$ as a function of temperature.

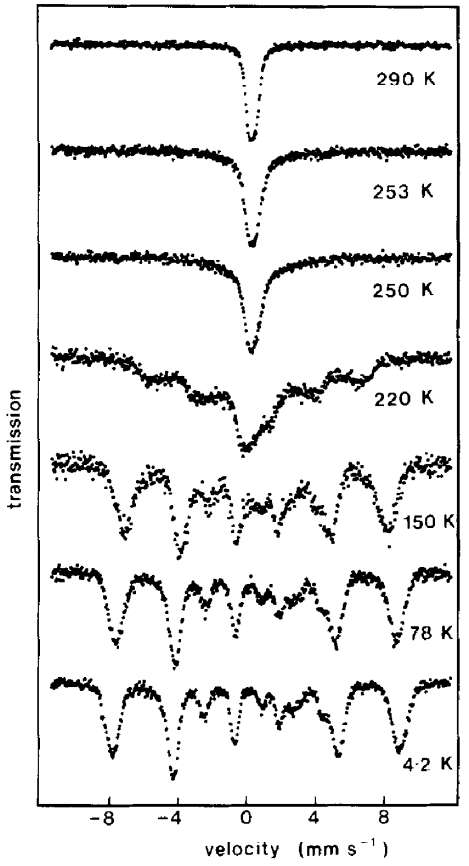

FIG. 8. The Mössbauer spectrum of $Ba_{0.5}La_{0.5}FeO_{2.970}$ as a function of temperature.

a significant change in the temperature at which hyperfine interactions appear, being circa 160 K ($x = 0.33$), 90 ($x = 0.20$), and 170 K ($x = 0.10$). We have already shown (*11*) that an increase in the vacancy concentration in $Sr_2LaFe_3O_{8+y}$ causes a large depression in the apparent ordering temperature. In the present case we would have to consider the simultaneous effects of changes in x and y, and although there appears to be a strong correlation between the ordering temperature and the value of y, we have not pursued the point further because of the disproportionate effort involved. Figures 5–8 show clearly that the electronic state of the iron in the paramagnetic state remains essentially unchanged as a function of temperature, although the much broader profiles for $x = 0.10$, 0.20, and 0.33 make a detailed computer analysis difficult. Nevertheless it would seem that the onset of magnetic order and charge disproportionation are interconnected.

Mössbauer Spectra of Samples Quenched into Liquid Nitrogen

The Mössbauer spectra at 290 K for samples quenched from 1300°C into liquid nitrogen are shown in Fig. 9. For $x < 0.5$ the compositions lie close to the fully reduced $Ba_2Fe_2O_5$–$LaFeO_3$ line (i.e., all Fe^{3+}). The

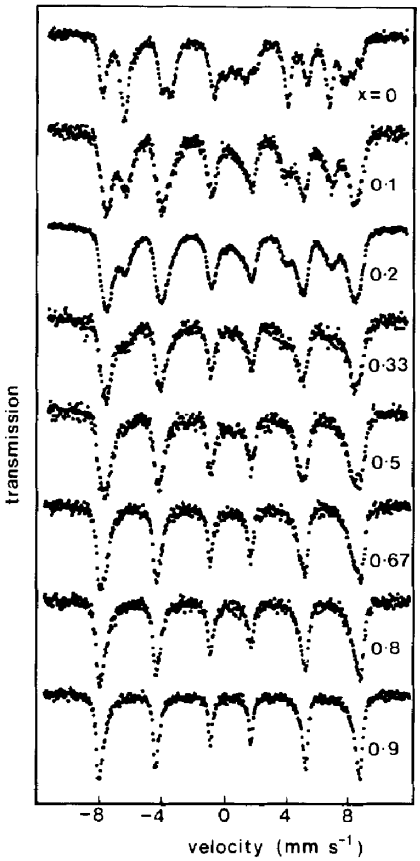

FIG. 9. The Mössbauer spectrum at 290 K for samples of $Ba_{1-x}La_xFeO_{3-y}$ quenched into liquid nitrogen from 1300°C.

spectrum for $x = 0$ is typical of the monoclinic phase of $Ba_2Fe_2O_5$ (*20*). The spectrum can be related to the simpler brownmillerite spectra. The outermost line on the left of the spectrum is produced by Fe^{3+} ions in octahedral coordination to oxygen, although the corresponding line at the extreme right of the spectrum is clearly split into at least three components indicating a multiplicity of octahedral sites. The average flux density is about 48.8 T. The next outermost lines are from Fe^{3+} ions in tetrahedral coordination, the significantly smaller field with a flux density of 40.4 T being characteristic of the lower coordination.

The cubic phases ($x > 0$) also show clear evidence for both octahedral and tetrahedral iron sites, but the relative proportions of the latter decrease far more rapidly than the increasing oxygen content would predict. For $x = 0.33$, where the maximum concentration of tetrahedral sites can be estimated from the chemical analysis to be 29%, the computed figure is only some 18%. Indeed the tetrahedral sites have almost disappeared at $x = 0.50$ when a figure of 22% of the total sites might have been expected. Moreover at $x = 0.33$ there is a clear asymmetry in the outer lines which means that there are two (or more) hyperfine fields with different chemical shifts. This is distinctly different to the $Ca_2Fe_2O_5$–$LaFeO_3$ solid solution where it has been shown (*32*) that vacancies are fully ordered into tetrahedal sites within the same range of x, the concentration of five-coordinated sites being negligible.

The observed behavior for the Ba/La system is similar to our earlier observations (*13*) on the cubic phases of $Sr_2MFe_3O_8$ (M = Pr, Nd, Sm, Eu, Gd, Dy, Y) where the computed binomial probabilities for 6, 5, and 4 coordination with random vacancies of 49, 37, and 12%, respectively, were compared with the average tetrahedral site concentration in the seven compounds of 13%. For Ba/La with $x = 0.33$ the ratios computed from the experimental data for the same 3-field model are 54, 28, and 18%, respectively. We conclude that vacancy ordering to give extra tetrahedral sites becomes less favorable with increasing x in the Ba/La system, and that there is an increase in the number of five-coordinate sites. The tendency to defect ordering will increase with decreasing temperature, but we have already shown that kinetic considerations may prevent ordering in the Sr/M systems (*12*). It remains a possibility that long annealing times at the correct temperature could induce some degree of ordering for Ba/La also.

For $x > 0.50$ the spectra gradually sharpen toward that of $LaFeO_3$. There are fewer oxygen vacancies, but there is no direct evidence for the proportion of iron in a higher oxidation state which the analysis requires. We have not investigated this region of the $Ba_{1-x}La_xFeO_{3-y}$ system in greater detail.

A series of samples with $x = 0.33$ were prepared by quenching into liquid nitrogen from different temperatures. The oxygen analyses and X-ray lattice parameters for the cubic phases produced are given in Table IV, and the Mössbauer spectra at 290 K are given in Fig. 10 and at 78 K in Fig. 11.

TABLE IV

THE OXYGEN PARAMETER y AND X-RAY LATTICE PARAMETER a FOR THE SOLID SOLUTIONS $Ba_{1-x}La_xFeO_{3-y}$ QUENCHED INTO LIQUID NITROGEN FROM DIFFERENT TEMPERATURES

T (quench) (°C)	y	a (Å)
1300	0.290	3.979
1100	0.299	3.982
900	0.272	3.971
700	0.221	3.960
500	0.164	3.950
300	0.119	3.941
Slow-cooled	0.113	3.939

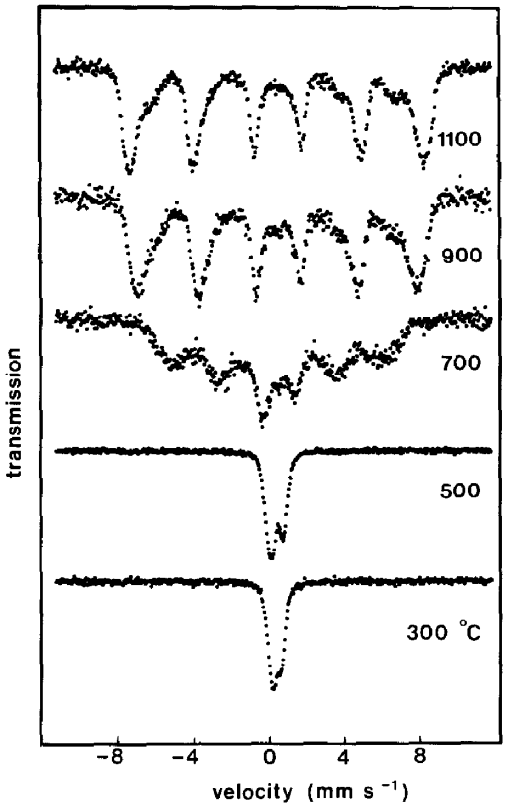

FIG. 10. The Mössbauer spectrum at 290 K for samples of $Ba_{0.67}La_{0.33}FeO_{3-y}$ quenched into liquid nitrogen from different temperatures.

As with $Sr_2LaFe_3O_{8+y}$ (*12*), the oxygen content increases steadily with decreasing temperature. The X-ray lines are sharp, and the large decrease in a and consequent movement of the high-angle reflections suggest that the materials remain single phase throughout the composition range. The Mössbauer spectra at 290 K for the 700°C quench is uniquely different compared to the 900 and 500°C quenches, consistent with this interpretation. The temperature for magnetic order falls dramatically as oxidation takes place. Magnetic hyperfine splitting appeared at circa 215 and 165 K for the 500 and 300°C quenches, respectively, compared to circa 160 K for the slow-cooled sample and above 290 K for the 900°C quench. From Figs. 7 and 11 it would appear that charge disproportionation is just becoming evident in the 700°C quench ($y = 0.221$).

The sample with $x = 0.33$ was further heated *in vacuo* at 1000°C. The resulting analysis of $Ba_2LaFe_3O_{8.057}$ and X-ray lattice parameter $a = 3.981$ Å suggested that the oxygen content was genuinely lower than for the original 1300°C quench into liquid nitrogen, but the material remained black. The Mössbauer spectrum was measured in an evacuated furnace, and revcalcd a straightforward Brillouin collapse without relaxation below an ordering temperature of $T_N = 705 \pm 2$ K.

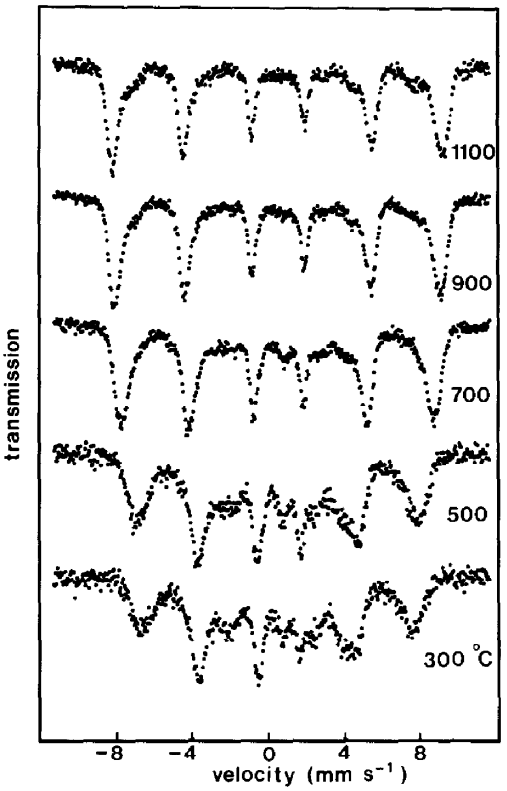

FIG. 11. The Mössbauer spectrum at 78 K for samples of $Ba_{0.67}La_{0.33}FeO_{3-y}$ quenched into liquid nitrogen from different temperatures.

Discussion

The observation of charge disproportionation in $Ba_{1-x}La_xFeO_{3-y}$ for a wide range of values of x and y is consistent with the similar behavior observed in related Ca and Sr iron oxides as detailed above. The noticeable exception is the $SrFeO_{3-y}$ system. $SrFeO_3$ which is a cubic metallic antiferromagnet shows a single hyperfine field with a flux density of 33.1 T at 4.2 K (*31*). Although there has been much discussion regarding the electronic state of the iron, the evidence (*11*) seems to favor a high-spin ($t_{2g}^3e_g^1$, $S = 2$) configuration, with metallic conductivity arising from a delocalized σ^* band derived from the e_g electronic states and thereby preventing a Jahn–Teller distortion. Loss of oxygen produces a series of ordered defect phases which show various combinations of effective oxidation states for the iron (*22, 33–35*), with averaged electron states at higher temperatures, but no evidence at all for the existence of Fe^{5+}.

It seemed reasonable to predict that charge disproportionation would be accompanied by a lattice distortion. We have recently collected (*11*) neutron powder diffraction data at 5 K for $Sr_2LaFe_3O_{8.94}$ which is cubic at room temperature, and have obtained clear evidence that the low-temperature phase is a noncubic antiferromagnet. A full structure analysis will be published in due course. Similar work is in progress on appropriate Ba/La samples. In particular, we hope to determine how the 6H-structure accommodates the charge disproportionation.

The structural chemistry of the iron perovskites with mixed *A*-site cations and in particular their tendency to show microdomain behavior are very interesting. Although both the Ca/La and Sr/La systems readily produce ordered-vacancy structures, the remarkable sensitivity of the structural chemistry to the radius of the *A*-cation (*13*) over the whole Sr/rare-earth series was unexpected. We have been unable to prepare ordered-vacancy phases in the $Ba_{1-x}La_xFeO_{3-y}$ system; the cubic materials reported here appear to be analogous to the cubic phase of $Sr_2MFe_3O_{8+y}$ (M = Pr, Nd, Sm, Eu, Gd, Dy, and Y). This cubic phase is believed to have a macroscopic perovskite lattice in which oxygen vacancies may be partially ordered into alternate FeO_2 layers to form a coherent intergrowth of small microdomains of a doubled perovskite cell in three orthogonal directions. The good structural coherence of the iron cation sublattice throughout a particle despite the presence of the microdomains leads to a coherence of the spin interactions and a unique Néel temperature without any significant spin relaxation effects. This cubic phase is thermodynamically unstable at low temperatures with respect to an orthorhombic phase with vacancies ordered into every third layer (as found in $Sr_2LaFe_3O_8$), but for kinetic reasons such an ordered phase is not always achieved. We have also been able to prepare a sample of $Sr_2LaFe_3O_8$ which gave X-ray evidence of a perovskite cell doubled along one edge, i.e., with a much larger domain size.

The recent work of Parras *et al.* (*14*) has shown that air-quenched $Ba_{1-x}La_xFeO_{3-y}$ samples, which are cubic to X-ray diffraction, may have a doubled perovskite cell when examined by electron diffraction with a shorter resolving wavelength. This applied to $x = 0.66$. Their failure to observe such a feature for $x < 0.66$ may reflect the nonequilibrium nature of samples which have rapidly taken up oxygen during the quench in air, and it would be interesting to repeat the study on annealed material. The low vacancy concentration of their $x = 0.66$ sample led them to postulate that the doubling of the unit cell is due to Ba/La ordering. It remains to be seen whether this explanation is also appropriate to the Sr/M systems. However, a similar microdomain behavior has been clearly established in $SrFe_{0.9}V_{0.1}O_{2.6}$ (*36*) where there is only one type of *A* cation but a large vacancy con-

centration. Our observation (*12*) of a diffuse reflection at a *d*-spacing of ~5.5 Å in both the orthorhombic and doubled-cell forms of $Sr_2LaFe_3O_8$ could be a result of short-range positional ordering of the *A* cations, ordering of the oxygen vacancies, or a combination of both. However, the same diffuse scattering is seen in the cubic $Ba_{1-x}La_xFeO_{3-y}$ materials despite the almost identical scattering of X-rays from Ba and La. This suggests that a simple positional ordering of the *A*-cations is not responsible, and that the effect is associated with the ordering of oxygen vacancies.

Acknowledgments

We thank the SERC for financial support, the Ramsay Memorial Fellowships Trust for a Fellowship (to M.M.), and Mr. A. Hedley for the chemical analyses.

References

1. M. K. Wu, J. R. Asburn, C. J. Torng, C. J. Hor, R. L. Meng, L. Gao, Z. J. Huang, Y. K. Wang, and C. W. Chu, *Phys. Rev. Lett.* **58,** 908 (1987).
2. J. C. Grenier, J. Darriet, M. Pouchard, and P. Hagenmuller, *Mater. Res. Bull.* **11,** 1219 (1976).
3. J. C. Grenier, F. Menil, M. Pouchard, and P. Hagenmuller, *Mater. Res. Bull.* **12,** 79 (1977).
4. J. C. Grenier, L. Fournes, M. Pouchard, P. Hagenmuller, and S. Komornicki, *Mater. Res. Bull.* **17,** 55 (1982).
5. M. A. Alario-Franco, M. J. R. Henche, M. Vallet, J. M. G. Calbet, J. C. Grenier, A. Wattiaux, and P. Hagenmuller, *J. Solid State Chem.* **46,** 23 (1983).
6. M. A. Alario-Franco, J. M. Gonzalez-Calbet, M. Vallet-Regi, and J. C. Grenier, *J. Solid State Chem.* **49,** 219 (1983).
7. J. M. Gonzalez-Calbet, M. Vallet-Regi, and M. A. Alario-Franco, *J. Solid State Chem.* **60,** 320 (1985).
8. P. D. Battle, T. C. Gibb, and S. Nixon, *J. Solid State Chem.* **73,** 330 (1988).
9. T. C. Gibb, *J. Solid State Chem.* **74,** 176 (1988).
10. J. C. Grenier, N. Ea, M. Pouchard, and P. Hagenmuller, *J. Solid State Chem.* **58,** 243 (1985).
11. P. D. Battle, T. C. Gibb, and S. Nixon, *J. Solid State Chem.* **77,** 124 (1988).
12. P. D. Battle, T. C. Gibb, and S. Nixon, *J. Solid State Chem.* **79,** 75 (1989).
13. P. D. Battle, T. C. Gibb, and S. Nixon, *J. Solid State Chem.* **79,** 86 (1989).
14. M. Parras, M. Vallet-Regi, J. M. Gonzalez-Calbet, M. Alario-Franco, and J. C. Grenier, *J. Solid State Chem.* **74,** 110 (1988).
15. H. J. Van Hook, *J. Phys. Chem.* **68,** 3786 (1964).
16. P. K. Gallagher, J. B. MacChesney, and D. N. E. Buchanan, *J. Chem. Phys.* **43,** 516 (1965).
17. J. B. MacChesney, J. F. Potter, R. C. Sherwood, and H. J. Williams, *J. Chem. Phys.* **43,** 3317 (1965).
18. S. Mori, *J. Amer. Ceram. Soc.* **49,** 600 (1966).
19. S. Mori, *J. Phys. Soc. Japan* **28,** 44 (1970).
20. T. Ichida, *J. Solid State Chem.* **7,** 308 (1973).
21. M. Zanne and C. Gleitzer, *Bull. Soc. Chim. Fr.,* 1567 (1971).
22. Y. Takeda, K. Kanno, T. Takada, O. Yamamoto, M. Takano, N. Nakayama, and Y. Bando, *J. Solid State Chem.* **63,** 237 (1986).
23. A. J. Jacobson, *Acta Crystallogr. Sect. B* **32,** 1087 (1976).
24. J. L. Hutchinson and A. J. Jacobson, *J. Solid State Chem.* **20,** 417 (1977).
25. E. Luccini, S. Meriani, and D. Minicelli, *Acta Crystallogr. Sect. B* **29,** 1217 (1973).
26. M. Parras, M. Vallet-Regi, J. M. Gonzalez-Calbet, M. A. Alario-Franco, J. C. Grenier, and P. Hagenmuller, *Mater. Res. Bull.* **22,** 1413 (1987).
27. S. Geller and E. A. Wood, *Acta Crystallogr.* **9,** 563 (1956).
28. M. Takano, N. Nakanishi, Y. Takeda, S. Naka, and T. Takada, *Mater. Res. Bull.* **12,** 923 (1977).
29. S. Komornicki, L. Fournes, H. C. Grenier, F. Menil, M. Pouchard, and P. Hagenmuller, *Mater. Res. Bull.* **16,** 967 (1981).
30. M. Takano, J. Kawachi, N. Nakanishi, and Y. Takeda, *J. Solid State Chem.* **39,** 75 (1981).
31. P. K. Gallagher, J. B. MacChesney, and D. N. E. Buchanan, *J. Chem. Phys.* **41,** 2429 (1965).
32. J. C. Grenier, L. Fournes, M. Pouchard, P. Hagenmuller, and S. Komornicki, *Mater. Res. Bull.* **17,** 55 (1982).
33. T. C. Gibb, *J. Chem. Soc. Dalton Trans.,* 1455 (1985).
34. L. Fournes, Y. Potin, J. C. Grenier, G. Demazeau, and M. Pouchard, *Solid State Commun.* **62,** 239 (1987).
35. M. Takano, T. Okita, N. Nakayama, Y. Bando, Y. Takeda, O. Yamamoto, and J. B. Goodenough, *J. Solid State Chem.* **73,** 140 (1988).
36. N. Nakayama, M. Takano, S. Inamura, N. Nakanisho, and K. Kosuge, *J. Solid State Chem.* **71,** 403 (1987).